

Break a Lag: Triple Exponential Moving Average for Enhanced Optimization

Roi Peleg¹, Yair Smadar¹, Teddy Lazechnik^{2,3}, Assaf Hoogi¹

¹The School of Computer Science, Ariel University, Israel

²Department of Mathematics, Ariel University, Israel

³University College London, London, UK

assafh@ariel.ac.il

Abstract

The performance of deep learning models is critically dependent on sophisticated optimization strategies. While existing optimizers have shown promising results, many rely on first-order Exponential Moving Average (EMA) techniques, which often limit their ability to track complex gradient trends accurately. This fact can lead to a significant lag in trend identification and suboptimal optimization, particularly in highly dynamic gradient behavior. To address this fundamental limitation, we introduce Fast Adaptive Moment Estimation (FAME), a novel optimization technique that leverages the power of Triple Exponential Moving Average. By incorporating an advanced tracking mechanism, FAME enhances responsiveness to data dynamics, mitigates trend identification lag, and optimizes learning efficiency. Our comprehensive evaluation encompasses different computer vision tasks including image classification, object detection, and semantic segmentation, integrating FAME into 30 distinct architectures ranging from lightweight CNNs to Vision Transformers. Through rigorous benchmarking against state-of-the-art optimizers, FAME demonstrates superior accuracy and robustness. Notably, it offers high scalability, delivering substantial improvements across diverse model complexities, architectures, tasks, and benchmarks.

1. Introduction

Optimization techniques play a pivotal role in advancing computer vision by enabling models to learn efficiently from data through loss function minimization. As the complexity of visual tasks—such as object detection, image segmentation, and fine-grained classification—continues to escalate, the ability of optimizers to balance computational efficiency with performance accuracy becomes increasingly paramount. Optimization methods for deep learning have evolved by addressing specific challenges in computer vision training.

Stochastic Gradient Descent (SGD) [27] laid the foundation for modern optimization techniques by scaling gradients

uniformly across all parameters. A significant advancement came with the introduction of Momentum [24] to SGD, facilitating smoother descent trajectories and accelerating convergence by accumulating past gradient information. However, the computational intensity of SGD, particularly in the high-dimensional spaces characteristic of computer vision problems, remained a critical obstacle. To address this issue, researchers developed adaptive learning rate methods, which use nonuniform step sizes to scale the gradient during training [22]. These adaptive first-order methods compute individualized learning rates for each parameter, offering improved convergence in complex loss landscapes. Notable examples include AdaDelta [38], which utilizes a moving window of past gradient updates; AdaGrad [5], which normalizes gradients based on their historical magnitudes; RMSProp [32], which addresses AdaGrad’s diminishing learning rate issue; and Adam [12], which combines the strengths of RMSProp with momentum by applying an exponential moving average (EMA) to past gradients and squared gradients. Subsequent variants have further refined these approaches. AMSGrad [25] ensures a non-increasing step size to enhance stability in non-convex optimization landscapes. AdaBound [21] dynamically bounds learning rates to mitigate the convergence issues of adaptive methods. AdamW [20] decouples weight decay from the optimization step, improving generalization in image classification tasks. AdaHessian [34] incorporates second-order information to navigate complex loss surfaces more effectively.

Despite faster convergence, EMA-based optimizers often track gradients non-optimally, compromising performance and generalization compared to SGD in vision tasks. This generalization gap has prompted research into hybrid approaches, such as SWATS [11], which alternates between SGD and Adam, and Mixing Adam and SGD (MAS) [14], which combines their update rules using constant factors. However, these fusion strategies have shown limited performance gains, failing to fully bridge the gap between adaptive methods’ fast initial progress and SGD’s superior generalization.

We propose FAME, a novel optimizer leveraging Triple Exponential Moving Average (TEMA) to address the fundamental limitations of current first-order EMA-based optimization methods.

Our key contributions include:

- **High-Order Optimization Framework:** FAME is the first optimizer to leverage Triple Exponential Moving Average (TEMA) for deep learning optimization. Unlike traditional first-order EMA-based methods, FAME’s hierarchical multi-level structure enables improved optimization.
- **Addressing Limitations of traditional EMA-based Optimizers:** FAME introduces a better mechanism for handling gradient dynamics through precise gradient tracking with minimal lag, stable training in noisy environments, and accelerated convergence for large-scale vision tasks.
- **Comprehensive Validation:** Experiments across 30 neural models, a diversity of vision tasks and five public benchmarks demonstrate FAME’s consistent superiority in accuracy, robustness, and training efficiency - compared with commonly used optimizers.

2. FAME: Fast-Adaptive Moment Estimation

2.1. EMA: A Foundation for Trend Analysis

EMA enables temporal data analysis. At its core, EMA implements a theoretically grounded weighting scheme that decays exponentially over time, and balances noise reduction and trend preservation. This mathematical foundation sets it apart from conventional smoothing operators, particularly Gaussian kernels, by minimizing temporal lag while maintaining signal fidelity.

Formally, let $x = x_{1:t} \in \mathbb{R}^t$ represents a temporal sequence up to time step t . EMA can be elegantly expressed through a recursive formulation:

$$\begin{aligned} \text{EMA}(x_{1:t}) &= \beta \cdot \text{EMA}(x_{1:t-1}) + (1 - \beta) \cdot x_t \\ &= (1 - \beta) \sum_{i=0}^t \beta^i x_{t-i}, \end{aligned} \quad (1)$$

EMA relies on its smoothing coefficient $\beta \in [0, 1]$, which forces a critical trade-off: small β values allow quick adaptation but amplify noise, while large β values reduce noise but introduce significant delays. This means first-order EMA must always sacrifice either speed or stability.

Although first-order EMA’s exponentially decaying memory structure helps stabilize gradient estimates, it fundamentally suffers from two problems: it lags behind actual changes and tends to over-smooth important gradient patterns. These issues can significantly impact optimization performance, especially in complex deep learning tasks.

Higher-order EMA techniques systematically address these limitations. By using multiple levels of exponential smoothing, they can achieve both quick adaptation and noise reduction - capabilities that are mathematically impossible with first-order EMA’s single smoothing coefficient (illustrated in Figure 1).

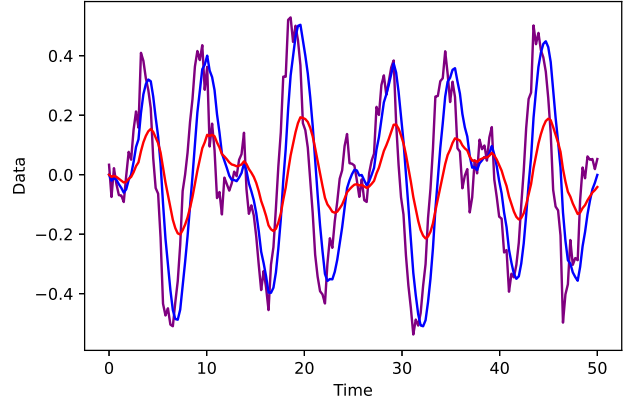


Figure 1. Simulated demonstration of gradient trend estimation and lagging. Ground truth (GT, purple), triple exponential moving average (TEMA)-based estimation (blue), and exponential moving average (EMA)-based estimation (red).

2.2. Double Exponential Moving Average (DEMA)

We introduce advanced smoothing techniques that address the inherent lag limitations of traditional Exponential Moving Averages (EMA). The Double Exponential Moving Average (DEMA) incorporates a lag-correction mechanism through:

$$\text{DEMA}(x) = 2\text{EMA}_1(x) - \text{EMA}_2(x) \quad (2)$$

where $\text{EMA}_k(x)$ represents k recursive applications of EMA:

$$\text{EMA}_k(x) = \underbrace{\text{EMA}(\text{EMA}(\dots \text{EMA}(x)))}_{k \text{ times}} \quad (3)$$

The key innovation in DEMA lies in its lag-correction term $[\text{EMA}_1(x) - \text{EMA}_2(x)]$, which provides a robust estimation of the temporal displacement between raw data x and its primary smooth estimate $\text{EMA}_1(x)$. This formulation enables DEMA to achieve superior temporal responsiveness while preserving signal fidelity.

2.3. Triple Exponential Moving Average (TEMA)

Building upon DEMA’s foundation, the Triple Exponential Moving Average (TEMA) introduces a second-order correction mechanism:

$$\text{TEMA}(x) = 3\text{EMA}_1(x) - 3\text{EMA}_2(x) + \text{EMA}_3(x) \quad (4)$$

TEMA formulation emerges from a hierarchical lag correction process:

$$\begin{aligned}
\text{TEMA}(x) &= \text{EMA}_1(x) + [\text{EMA}_1(x) - \text{EMA}_2(x)] \\
&+ [(\text{EMA}_1(x) - \text{EMA}_2(x)) - \text{EMA}(\text{EMA}_1(x) - \text{EMA}_2(x))] \\
&= \text{EMA}_1(x) + [\text{EMA}_1(x) - \text{EMA}_2(x)] \\
&+ [\text{EMA}_1(x) - 2\text{EMA}_2(x) + \text{EMA}_3(x)] \\
&= 3\text{EMA}_1(x) - 3\text{EMA}_2(x) + \text{EMA}_3(x) \tag{5}
\end{aligned}$$

The formulation consists of three critical components: (1) the initial smooth estimate $\text{EMA}_1(x)$, (2) the first-order lag correction $[\text{EMA}_1(x) - \text{EMA}_2(x)]$, and (3) the second-order refinement term $[\text{EMA}_1(x) - 2\text{EMA}_2(x) + \text{EMA}_3(x)]$. This hierarchical structure enables TEMA to achieve unprecedented adaptability to temporal dynamics while maintaining signal coherence.

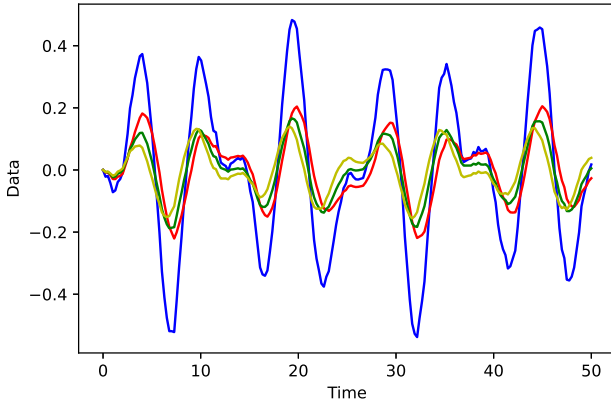


Figure 2. Decomposition of TEMA (blue) into its constituent components: EMA_1 (red), first-order correction ($\text{EMA}_1 - \text{EMA}_2$) (green), and second-order correction ($\text{EMA}_1 - 2\text{EMA}_2 + \text{EMA}_3$) (yellow). The composite TEMA signal demonstrates the synergistic integration of these components.

As visualized in Figure 2, TEMA’s components exhibit distinct phase characteristics that, when combined, achieve optimal lag reduction while preserving signal integrity. The complementary nature of these components enables robust temporal adaptation across diverse signal dynamics.

2.4. Generalized k-th Order Exponential Moving Average

We further generalize this framework to arbitrary orders through the k-th order EMA formulation:

$$\text{KEMA}_k(x) = \sum_{i=1}^k (-1)^{i+1} \binom{k}{i} \text{EMA}_i(x) \tag{6}$$

This generalization provides fine-grained control over the temporal responsiveness-smoothness trade-off, enabling

optimal adaptation to specific optimization scenarios. The binomial coefficients in this formulation ensure proper weighting of higher-order corrections, maintaining mathematical consistency with lower-order variants.

2.5. FAME Intuition

This section provides better intuition and deeper insights into FAME’s mechanisms and advantages, building upon the presented mathematical foundations.

EMA is a fundamental smoothing technique that weights sequential data, assigning higher importance to recent values while exponentially diminishing the influence of older ones. This creates a local window that naturally emphasizes current patterns while maintaining historical context. When applied recursively—calculating EMA on an already smoothed signal ($\text{EMA}(\text{EMA})$)—the smoothing effect compounds hierarchically. The first-level EMA captures immediate trends based on its smoothing factor, while subsequent EMAs further refine this signal, effectively expanding the observation window and enabling more sophisticated pattern detection. Building upon this foundation, FAME introduces three key innovations:

1. **Advanced Multi-Scale Optimization:** Traditional first-order EMA optimizers face a fundamental speed-stability dilemma: shorter windows offer quick adaptation but amplify noise, while longer windows ensure stability at the cost of responsiveness. FAME transcends this limitation through its hierarchical triple-EMA structure. The three interconnected EMA levels form a cascading filtering pyramid, where each level operates at progressively longer time scales: the first captures immediate gradient dynamics, the second aggregates emerging patterns, and the third maintains stable long-term momentum.
2. **Smarter Trend Recognition:** First-order EMA simply follows past gradients data, making it slow to recognize new trends. TEMA’s three-level mechanism acts like a verification chain: the first level spots potential changes, the second level confirms them, and the third level validates their importance. This helps it quickly identify real trends while ignoring temporary fluctuations.
3. **Quick Error Correction:** When first-order EMA makes a mistake, it takes time to recover. TEMA’s structure allows for faster error correction because each level helps compensate for errors in the others.

FAME’s nature makes Triple EMA especially valuable in deep learning optimization, where we need to quickly and accurately respond to changes in the model’s behavior while maintaining stable training.

2.6. Formulation of FAME

Let $f(\theta)$ be a differentiable stochastic scalar function that depends on the parameters θ . It is a noisy version of the expected objective function $F(\theta) = \mathbb{E}[f(\theta)]$. Our goal is to minimize $F(\theta)$ with respect to its parameters θ , given only a sequence $f_1(\theta), \dots, f_T(\theta)$ of realizations of the stochastic function f at subsequent time steps $1, \dots, T$. The stochasticity in f may originate from evaluations on random subsamples of data points or from inherent function noise.

2.6.1. Gradient Estimation

The gradient, i.e., the vector of partial derivatives of f_t with respect to θ , evaluated at time step t , is denoted by:

$$g_t = \nabla_{\theta} f_t(\theta) \quad (7)$$

2.6.2. Moment Estimation

Similar to Adam, FAME tracks the first-order and second-order moments (m_t, v_t) of the gradients using an exponential moving average (EMA):

$$\begin{aligned} m_t &= \beta_1 m_{t-1} + (1 - \beta_1) g_t \\ v_t &= \beta_2 v_{t-1} + (1 - \beta_2) g_t^2 \end{aligned} \quad (8)$$

where the hyperparameters $\beta_1, \beta_2 \in [0, 1)$ control the exponential decay rates of these moving averages.

FAME extends beyond traditional optimizers by incorporating higher-order moment estimations. It tracks additional variables (dm_t, dv_t) for estimating EMA₂:

$$\begin{aligned} dm_t &= \beta_3 dm_{t-1} + (1 - \beta_3) m_t \\ dv_t &= \beta_4 dv_{t-1} + (1 - \beta_4) v_t \end{aligned} \quad (9)$$

Based on (dm_t, dv_t) , FAME further estimates EMA₃ using variables (tm_t, tv_t) :

$$\begin{aligned} tm_t &= \beta_5 tm_{t-1} + (1 - \beta_5) dm_t \\ tv_t &= \beta_4 tv_{t-1} + (1 - \beta_4) dv_t \end{aligned} \quad (10)$$

Here, (m_0, v_0) , (dm_0, dv_0) , and (tm_0, tv_0) are all initialized to 0.

Incorporating Eqs. (8-10) into the Triple Exponential Moving Average (TEMA) equation (Eq. 4) yields:

$$\begin{aligned} m_{\text{FAME}_t} &= 3m_t - 3dm_t + tm_t \\ v_{\text{FAME}_t} &= 3v_t - 3dv_t + tv_t \end{aligned} \quad (11)$$

2.6.3. Parameter Update Rule

The final parameter update equation for FAME is given by:

$$\theta_t = \theta_{t-1} - \alpha \cdot \frac{m_{\text{FAME}_t}}{\sqrt{v_{\text{FAME}_t} + \epsilon}} \quad (12)$$

where α is the learning rate and ϵ is a small constant to prevent division by zero.

3. Experiments

We validated the FAME optimizer across five diverse benchmarks and 30 model models with varying complexities, covering tasks like detection, classification, and semantic understanding. FAME was compared against six popular optimizers: SGD + Momentum, Adam, Adagrad, AdamW, AdaBound, and AdaHessian.

Algorithm 1: FAME Optimizer

Input: Hyper-parameters: $\beta_1, \beta_2, \beta_3, \beta_4, \beta_5, \alpha, \epsilon$

Output: Optimized parameters θ_t after convergence

```

1 Initialize:  $m_0 \leftarrow 0, v_0 \leftarrow 0, dm_0 \leftarrow 0, dv_0 \leftarrow 0,$ 
    $tm_0 \leftarrow 0, tv_0 \leftarrow 0, t \leftarrow 0$ 
2 while  $\theta_t$  not converged do
3    $t \leftarrow t + 1$ 
4    $m_t \leftarrow \beta_1 m_{t-1} + (1 - \beta_1) g_t$ 
5    $v_t \leftarrow \beta_2 v_{t-1} + (1 - \beta_2) g_t^2$ 
6    $dm_t \leftarrow \beta_3 dm_{t-1} + (1 - \beta_3) m_t$ 
7    $dv_t \leftarrow \beta_4 dv_{t-1} + (1 - \beta_4) v_t$ 
8    $tm_t \leftarrow \beta_5 tm_{t-1} + (1 - \beta_5) dm_t$ 
9    $tv_t \leftarrow \beta_4 tv_{t-1} + (1 - \beta_4) dv_t$ 
10   $m_{\text{FAME}_t} \leftarrow 3m_t - 3dm_t + tm_t$ 
    $v_{\text{FAME}_t} \leftarrow 3v_t - 3dv_t + tv_t$ 
11   $\theta_t \leftarrow \theta_{t-1} - \alpha \cdot \frac{m_{\text{FAME}_t}}{\sqrt{v_{\text{FAME}_t} + \epsilon}}$ 
12 end
13 return  $\theta_t$ 

```

3.1. Experimental Data

We tested our proposed FAME on five public benchmarks: CIFAR-100 [13], MS-COCO [17], PASCAL-VOC [6], Cityscapes [2], and the large scale ImageNet [28].

3.2. Implementation Details

To ensure a rigorous comparison, all optimizers were evaluated under identical initialization conditions and trained from scratch. While this approach may yield lower absolute accuracies compared to pre-trained models, it enables an unbiased assessment of each optimizer’s intrinsic capabilities. For fair comparison, we conducted comprehensive hyperparameter tuning for each optimizer, starting from literature-recommended defaults and employing grid search to identify optimal settings. Given FAME’s extensive validation across 30 models, we follow standard practice by referencing the established hyperparameter configurations from prior work for each model.

4. Results

In pursuit of a comprehensive analysis, we computed several statistical metrics, including accuracy, mAP (mean Average Precision), precision, recall, and F1-score. This involved

evaluating the average and standard deviation across three distinct model initializations, solidifying the robustness of our method’s validation.

4.1. Image Classification

4.1.1. CIFAR-100

FAME demonstrates superior performance on CIFAR-100 across 17 diverse models (Table 1). When compared with commonly used optimizers, FAME achieved superior accuracy in 84.6% of the models, consistently outperforming existing methods with averaged accuracy improvements of 1.16% over AdamW, 1.57% over AdaBound, 3.52% over AdaHessian, and 16.33% over AdaGrad.

Beyond accuracy gains, FAME demonstrated superior training stability across diverse models. For CNN-based models, FAME reduced epoch-wise accuracy variance by 29.27% compared with existing optimizers (Adam, SGD, AdamW, AdaBound, AdaHessian, AdaGrad). This stability advantage persisted in transformer-based models, where FAME achieves a 21.54% variance reduction compared with the same baseline optimizers. Such consistent stability across different models highlights FAME’s robustness to gradient dynamics, effectively mitigating the training fluctuations common in current methods.

4.1.2. ImageNet Benchmark

Our ImageNet experiments reveal FAME’s compelling advantages across models. For CNN-based models, FAME achieved consistent accuracy improvements of 0.8% over Adam and 0.65% over SGD. The gains were even more pronounced in Transformer-based models, where FAME surpassed Adam by 0.97% and SGD by 1.27%. Beyond accuracy improvements, FAME enhanced the training process in two critical aspects. First, it provided superior training stability, reducing accuracy fluctuations variance by 5.64% compared with SGD, Adam, and AdamW. Second, it accelerated convergence significantly, reaching 90% of peak accuracy while using only 78% of the epochs required by other optimizers. This comprehensive enhancement in accuracy, stability, and training efficiency establishes FAME as a powerful optimization solution for large-scale vision tasks.

4.2. Object Detection

4.2.1. MS-COCO Benchmark

Table 2 demonstrates FAME’s effectiveness on the MS-COCO benchmark using YOLOv5-S model, where it consistently outperforms standard optimizers including SGD, Adam, and AdamW. FAME achieved a mean Average Precision (mAP@0.5) of 0.569, surpassing SGD (0.549), Adam (0.265), and AdamW (0.446), and also excelled in mAP@0.5:0.95 with a score of 0.375 compared to 0.352 for SGD, 0.211 for Adam, and 0.271 for AdamW. In terms

of Precision, FAME scored 0.663, indicating a high proportion of true positives, while Recall was at 0.521, showcasing its effectiveness in capturing relevant objects. Additionally, FAME’s F1-Score of 0.583 reflects a strong balance between precision and recall, significantly outperforming SGD (0.518), Adam (0.275), and AdamW (0.471). Overall, these results affirm FAME’s enhanced object detection capabilities, positioning it as a robust optimization method in comparison to established techniques.

4.2.2. Pascal-VOC Benchmark

Table 3 presents the analysis of the Pascal Visual Object Classes (VOC) dataset for detection and classification tasks, highlighting FAME’s advantages over conventional optimizers like SGD, Adam, and AdamW. For the YOLOv5-S model, FAME achieved a mean Average Precision (mAP) of 0.812, which exceeds the performance of SGD (0.787), Adam (0.651), and AdamW (0.801). Similarly, FAME recorded an impressive mAP of 0.851 for the YOLOv5-m model, compared with SGD (0.828), Adam (0.662), and AdamW (0.83). In classification using the RevViT model, FAME reached an AUC score of 0.696, surpassing SGD (0.679), Adam (0.637), and AdamW (0.671). These findings demonstrate that FAME consistently enhances performance in both detection and classification tasks, underscoring its efficacy as an optimization technique relative to commonly used methods.

4.3. Semantic Segmentation

4.3.1. Cityscapes Benchmark

Our evaluation of the Cityscapes benchmark demonstrates FAME’s consistent superiority across diverse models (Table 4). FAME achieved the highest accuracy in 6 out of 7 models (85.7%), with improvements ranging from 0.3% to 1% over Adam and 2.5% to 6.3% over SGD. Notably, FAME showed particularly strong performance on resource-efficient models like MobileNetV2 (+0.7% over Adam, +6.3% over SGD) and more complex models like DL-V3+ResNet101 (+1.1% over Adam, +4.7% over SGD). The results also reveal FAME’s stability advantage, evidenced by consistently lower standard deviations across three initializations.

4.4. Robustness across Datasets, models, and Weight Initializations

Tables 1-4 show that for 87.16% of the models, FAME outperforms all the other optimizers examined in this study, and its performance is comparable with those of the other optimizers for the remaining 12.9% cases. Thus, its high robustness within and across datasets was established. Furthermore, FAME demonstrated a lower standard deviation across the different weight initializations.

4.5. Ablation Study

- **Effect of High-Order EMAs** — Table 5 shows that increasing the order of the EMA from simple EMA to

Table 1. Image Classification. CIFAR-100 and Imagenet benchmarks. Comparison of classification accuracy (Mean \pm Std) supplied by different optimizers across models. **Best results for each model are bolded**. All SGD and Adam results are comparable to the literature results when training from *scratch*. Std was calculated for three different initializations. " L_{drloc} " signifies the addition of dense relative localization loss [18], which improves the robustness of visual transformers

Dataset	Type	model	Our FAME	Adam	SGD + Momentum
CIFAR-100	CNN	EfficientNet-b3 [31]	0.761 \pm 0.008	0.749 \pm 0.015	0.748 \pm 0.017
		EfficientNet-b5 [31]	0.793 \pm 0.010	0.776 \pm 0.016	0.771 \pm 0.017
		MobileNetV3-Large [8]	0.756 \pm 0.005	0.706 \pm 0.007	0.744 \pm 0.011
		DenseNet-121 [10]	0.738 \pm 0.008	0.714 \pm 0.015	0.727 \pm 0.011
		DenseNet-201 [10]	0.739 \pm 0.005	0.742 \pm 0.006	0.733 \pm 0.006
		SEResNet-18 [9]	0.715 \pm 0.009	0.704 \pm 0.009	0.692 \pm 0.016
		SE-ResNet-50 [9]	0.762 \pm 0.007	0.751 \pm 0.009	0.747 \pm 0.011
		Dspike (ResNet-18) [16]	0.723 \pm 0.006	0.708 \pm 0.008	0.693 \pm 0.019
		PyramidNet-272 [7]	0.832 \pm 0.006	0.811 \pm 0.008	0.808 \pm 0.008
		Inception-v3 [30]	0.751 \pm 0.006	0.743 \pm 0.008	0.702 \pm 0.015
		WideResNet 40-4 [37]	0.719 \pm 0.007	0.706 \pm 0.009	0.708 \pm 0.007
		Transformer	ViT-Base+ L_{drloc} [26]	0.743 \pm 0.003	0.739 \pm 0.002
	Swin-T+ L_{drloc} [19]		0.774 \pm 0.002	0.769 \pm 0.007	0.762 \pm 0.002
	CvT-13+ L_{drloc} [33]		0.795 \pm 0.001	0.794 \pm 0.001	0.780 \pm 0.005
T2T-ViT-14+ L_{drloc} [36]	0.781 \pm 0.003		0.783 \pm 0.001	0.806 \pm 0.002	
ImageNet	CNN	MobileNetV3-Large [8]	0.729 \pm 0.001	0.726 \pm 0.001	0.727 \pm 0.001
		EfficientNet-b5 [31]	0.785 \pm 0.016	0.772 \pm 0.014	0.774 \pm 0.016
	Transformer	CvT-13 [33]	0.824 \pm 0.009	0.820 \pm 0.010	0.819 \pm 0.016
		CAFormer-S18 [35]	0.848 \pm 0.010	0.835 \pm 0.013	0.833 \pm 0.012
		CAFormer-S36 [35]	0.869 \pm 0.010	0.857 \pm 0.013	0.851 \pm 0.012

Table 2. Object Detection. MS-COCO by YOLOv5-s [15]. Accuracy by Mean \pm Std. The Std was calculated over three initializations. The results match those of training from *scratch*, as reported in the literature.

	Our FAME	SGD	Adam	AdamW
mAP@0.5	0.569 \pm 0.003	0.549 \pm 0.005	0.265 \pm 0.021	0.446 \pm 0.013
mAP@0.5:0.95	0.375 \pm 0.003	0.352 \pm 0.005	0.211 \pm 0.021	0.271 \pm 0.014
Precision	0.663 \pm 0.009	0.658 \pm 0.011	0.332 \pm 0.013	0.542 \pm 0.011
Recall	0.521 \pm 0.006	0.427 \pm 0.006	0.234 \pm 0.019	0.417 \pm 0.007
F1-Score	0.583 \pm 0.008	0.518 \pm 0.012	0.275 \pm 0.014	0.471 \pm 0.004

Table 3. Pascal visual object classes (VOC) detection/classification. Std was calculated over three initializations. The results match those for training from *scratch* as reported in literature.

	Our Fame	SGD	Adam	AdamW
Yolov5-s [15] (mAP) - <i>Detection</i>	0.812 \pm 0.007	0.787 \pm 0.007	0.651 \pm 0.009	0.801 \pm 0.009
Yolov5-m [29] (mAP) - <i>Detection</i>	0.851 \pm 0.006	0.828 \pm 0.007	0.662 \pm 0.011	0.830 \pm 0.009
RevViT [4] (AUC) - <i>Classification</i>	0.696 \pm 0.006	0.679 \pm 0.007	0.637 \pm 0.009	0.671 \pm 0.007

DEMA, and then to TEMA, leads to improved model performance. Although the 4th order was also tested, it underperformed compared to TEMA, which balanced between trend estimation, smoothness and lag reduction. The results emphasize that our triple-based FAME consistently outperformed other high-order EMAs across various datasets, tasks, and models, delivering superior accuracy.

- **Effect of TEMA on Different Moments** — Table 6 illus-

Table 4. Semantic Segmentation. Cityscapes benchmark. "DL" - DeepLab [1]. Comparison of classification accuracy (Mean \pm Std) supplied by different optimizers across models. **Best results for each model are bolded.** All SGD and Adam results are comparable to the literature results when training from scratch. Std was calculated over three different initializations.

Model	Our FAME	Adam	SGD
DL-V3+HRNetV2-32	0.633 \pm 0.004	0.623 \pm 0.007	0.582 \pm 0.004
DL-V3+HRNetV2-48	0.641 \pm 0.009	0.634 \pm 0.011	0.609 \pm 0.007
DL-V3+ResNet50*	0.757 \pm 0.009	0.759 \pm 0.011	0.705 \pm 0.013
DL-V3+ResNet101*	0.778 \pm 0.009	0.767 \pm 0.014	0.731 \pm 0.012
DL-V3+MobileNetV2*	0.730 \pm 0.013	0.723 \pm 0.014	0.667 \pm 0.018
DL-V3+Xception	0.605 \pm 0.002	0.602 \pm 0.001	0.572 \pm 0.008
HANet-ResNet101*	0.836 \pm 0.001	0.833 \pm 0.001	0.817 \pm 0.013

trates how incorporating TEMA into the 1st and 2nd moments of FAME enhanced its performance. The shift from EMA to Partial TEMA (for 1st m_{FAME_t} moment only) and then to full FAME (for both m_{FAME_t} and v_{FAME_t} moments) consistently boosted accuracy. This demonstrates FAME’s capability to improve optimization across object detection, classification, and segmentation tasks, regardless of the dataset or model.

Table 5. Effect of the optimizer order

Dataset	Model	EMA	DEMA	Our FAME
CIFAR-100	ResNet34	0.721 \pm 0.008	0.727 \pm 0.006	0.736 \pm 0.006
		0.265 \pm 0.021	0.317 \pm 0.004	0.569 \pm 0.013
PASCAL-VOC	YOLOv5-m [29]	0.662 \pm 0.011	0.806 \pm 0.005	0.851 \pm 0.006
		0.743 \pm 0.008	0.751 \pm 0.005	0.757 \pm 0.005

Table 6. Ablation study. "Partial FAME" means using TEMA for M_{FAME_T} only, while "Our FAME" means using TEMA for both M_{FAME_T} and V_{FAME_T} . CIFAR100: ResNet50, MS-COCO: YOLOv5-s, Pascal-VOC: YOLOv5-m, and Cityscapes: ResNet50+DeepLabV3.

Dataset	Adam (Original EMA)	Partial FAME	Our FAME
CIFAR-100 (<i>Accuracy</i>)	0.721 \pm 0.008	0.729 \pm 0.005	0.736 \pm 0.006
MS-COCO (<i>mAP</i>)	0.265 \pm 0.021	0.504 \pm 0.006	0.569 \pm 0.013
PASCAL-VOC (<i>mAP</i>)	0.662 \pm 0.011	0.829 \pm 0.008	0.851 \pm 0.006
CityScapes (<i>mean IoU</i>)	0.743 \pm 0.008	0.751 \pm 0.005	0.757 \pm 0.005

4.6. Sensitivity to Hyper-parameters Tuning

4.6.1. FAME’s Hyper-parameter Robustness

While FAME introduces three additional parameters ($\beta_3, \beta_4, \beta_5$) beyond Adam’s β_1 and β_2 , it demonstrates remarkable stability. Across five major benchmarks, FAME shows only 3.72% performance variation compared to Adam’s 10.12% sensitivity - highlighting its robustness while delivering superior optimization. Notably, these parameters remained fixed across all experiments, eliminating the need for per-task tuning.

4.6.2. General Deep Model’s Hyper-parameters

To ensure fair evaluation, we performed comprehensive grid searches over all core hyperparameters (batch size, learning rate, momentum, weight decay, epochs) for each model, starting from established defaults and methodically exploring neighboring values - creating a robust foundation for meaningful comparisons.

4.7. Memory Cost and Computational Efficiency

Our assessment of FAME’s computational demands reveals a compelling efficiency trade-off:

1. *Per-Epoch Performance* – While FAME requires modestly higher resources per epoch (+7% memory, +5% computation time) compared to ADAM and SGD optimizers,
2. *Overall Efficiency* – FAME’s superior convergence characteristics dramatically offset these minor costs - achieving full convergence in just 76.3% of the training epochs required by traditional optimizers, averaged for all models and tested benchmarks.

This effectively means that FAME makes far better use of computational resources, requiring only about one-fifth

of the total training time despite slightly higher per-epoch overhead.

4.8. Convergence Analysis

To demonstrate the convergence of the proposed FAME algorithm, we begin by establishing a mathematical framework. Let $d \in \mathbb{N}$ represent the number of parameters in the function $F : \mathbb{R}^d \rightarrow \mathbb{R}$ that we aim to optimize. In the domain of machine learning, F embodies the complete training objective function, and optimization algorithms are employed to locate critical points within F . Specifically, our focus lies on optimization techniques that expand upon the classical Gradient Descent (GD) algorithm by integrating a heavy-ball style momentum parameter [23]. These algorithms exhibit a continuously diminishing step size from an initial finite step, leading to a monotonically decreasing process [12]. This behavior underscores their progression towards convergence.

Let us assume several constraints: $0 \leq \beta_5 \leq \beta_3 \leq \beta_1 \leq 1$ and $0 \leq \beta_4 \leq \beta_2 \leq 1$, along with the condition $\beta_1 \leq \beta_2$, and a non-negative value for α .

According to Algorithm 1, we define three sequences, $m_i, v_i, \theta_i \in \mathbb{R}^n$, where n denotes the dimension of the parameter space. Given an initial point $\theta_0 \in \mathbb{R}^n$ and setting $m_0 = v_0 = 0$, we proceed under three primary assumptions:

- The loss function F is bounded below by an arbitrary function F^* for any point $\forall \theta \in \mathbb{R}^n : F^*(\theta) \leq F(\theta)$.
- The loss function, concerning the max-norm (l_∞), is uniformly and surely bounded: $\forall \epsilon > 0, \exists r > \epsilon \forall \theta \in \mathbb{R}^n : \|\nabla F\|_\infty \leq r - \epsilon$.
- The loss function maintains L-Lipschitz continuity concerning the l_2 -norm: $\forall \theta, \zeta \in \mathbb{R}^n : \|\nabla F(\theta) - \nabla F(\zeta)\|_2 \leq L\|\theta - \zeta\|_2$.

For a specific number of iterations $N \in \mathbb{N}$, we introduce τ as a random index ranging from $\{0, \dots, N-1\}$, where $\forall i \in \mathbb{N} : i < N, P[\tau = i] \propto 1 - \beta_1^{N-i}$. This implies that for $\beta_1 = 0$, τ is uniformly sampled, while higher orders approaching zero lead to fewer samples in later iterations. This stratagem aims to limit the expected squared gradient norm at iteration τ .

For $N > \beta_1/(1 - \beta_1) \in \mathbb{N}$, the following inequality holds:

$$\begin{aligned} \|\nabla F(\theta_\tau)\|^2 &\leq 2r\sqrt{N} \frac{F(\theta_0) - F^*}{\alpha(N - \frac{\beta_1}{1-\beta_1})} + \\ &\frac{\sqrt{N}}{N - \frac{\beta_1}{1-\beta_1}} \ln \left(1 + \frac{Nr^2}{\epsilon} \right) \left(\alpha nrL + \frac{12dR^2}{1 - \beta_1} + \frac{2\alpha^2 dL^2 \beta_1}{1 - \beta_1} \right) \end{aligned} \quad (13)$$

Continuing with Algorithm 1, we can split the proof into two cases:

- When $\beta_3 = \beta_5 = \beta_4 = 0$, the algorithm adopts the form $\theta_t = \theta_{t-1} - \alpha \frac{m_t}{v_t}$, akin to the AdaGrad algorithm, known for convergence [3].
- For $\exists j \in \{3, 4, 5\} : \beta_j > 0$, dm_t, tm_5, dv_t , and tv_t depend on m_t and v_t , converging at some point following the first case. Thus, a $\delta \in \mathbb{N}$ emerges with $\epsilon \|\psi_\delta - \psi_{\delta-1}\|_2 \leq \epsilon^*$ for $\psi \in \{dm, tm, dv, tv\}$. Consequently, beyond this interaction (δ), the update rule transforms into $\forall t > \delta : \theta_t = \theta_{t-1} - \alpha \frac{m_t + c_1}{v_t + c_2}$, with $c_1, c_2 \in \mathbb{R}^n$. This update rule can be upper-bounded by a constant $c_3 \in \mathbb{R}^n$, resembling ADAgrad, because the adaptive update roughly aligns with the descent direction. Thus, the convergence at $\tau \in \mathbb{N}$ implies subsequent steps being smaller, bounded by ADAgrad convergence processes from the same initial configuration.

Ultimately, by establishing an upper limit to convergence in the second case, we demonstrate convergence in this scenario as well.

5. Conclusion

We introduced FAME, a novel optimization algorithm that utilizes TEMA to overcome the fundamental limitations of traditional EMA-based optimizers in accurately tracking gradient trends and mitigating optimization lag. Through extensive empirical evaluation across 30 architectures and a diverse range of computer vision tasks—encompassing classification, detection, and dense prediction—we demonstrated FAME’s high versatility, superior robustness, and adaptability. FAME outperformed state-of-the-art optimizers in 86.67% of evaluated models, consistently maintaining lower variance and stability under diverse conditions. Beyond delivering better performance, FAME demonstrated significant practical advantages by reducing average convergence time by 23.7%, enhancing training stability, and exhibiting performance less sensitive to specific model architectures or benchmark settings. This versatility underscores FAME’s potential as a reliable optimizer, especially in settings requiring scalability and model independence. With its theoretical basis in hierarchical EMA structures and demonstrated empirical superiority across model-benchmark configurations, FAME enables more efficient and resilient training across a broad spectrum of applications.

References

- [1] Liang-Chieh Chen, Yukun Zhu, George Papandreou, Florian Schroff, and Hartwig Adam. Encoder-decoder with atrous separable convolution for semantic image segmentation. *CoRR*, abs/1802.02611, 2018. 7
- [2] M. Cordts, M. Omran, S. Ramos, T. Rehfeld, M. Enzweiler, R. Benenson, U. Franke, S. Roth, and B. Schiele. The cityscapes dataset for semantic urban scene understanding. In *Proceedings of the IEEE conference on computer vision and pattern recognition*, pages 3213–3223, 2016. 4

- [3] A. Defossez, L. Bottou, F. Bach, and N. Usunier. A simple convergence proof of adam and adagrad. *Machine Learning Research*, 2022. 8
- [4] Anxhelo Diko, Danilo Avola, Marco Cascio, and Luigi Cinque. Revit: Enhancing vision transformers feature diversity with attention residual connections, 2024. 6
- [5] John Duchi, Elad Hazan, and Yoram Singer. Adaptive subgradient methods for online learning and stochastic optimization. *Journal of Machine Learning Research*, 12:2121–2159, 2011. 1
- [6] M. Everingham, S. M. A. Eslami, L. Van Gool, C. K. I. Williams, J. Winn, and A. Zisserman. The pascal visual object classes challenge: A retrospective. *International Journal of Computer Vision*, 111(1):98–136, 2015. 4
- [7] Dongyoon Han, Jiwhan Kim, and Junmo Kim. Deep pyramidal residual networks, 2017. 6
- [8] Andrew Howard, Mark Sandler, Grace Chu, Liang-Chieh Chen, Bo Chen, Mingxing Tan, Weijun Wang, Yukun Zhu, Ruoming Pang, Vijay Vasudevan, Quoc V. Le, and Hartwig Adam. Searching for mobilenetv3, 2019. 6
- [9] Jie Hu, Li Shen, Samuel Albanie, Gang Sun, and Enhua Wu. Squeeze-and-excitation networks, 2019. 6
- [10] Gao Huang, Zhuang Liu, Laurens van der Maaten, and Kilian Q. Weinberger. Densely connected convolutional networks, 2018. 6
- [11] N. S. Keskar and R. Socher. Improving generalization performance by switching from adam to sgd. *arXiv*, 2017. 1
- [12] Diederik P Kingma and Jimmy Ba. Adam: A method for stochastic optimization. *arXiv preprint arXiv:1412.6980*, 2014. 1, 8
- [13] A. Krizhevsky. Learning multiple layers of features from tiny images. *technical report*, pages 32–33, 2009. 4
- [14] N. Landro, I. Gallo, and R. L. Grassa. Mixing ADAM and SGD: a combined optimization method. *CoRR*, abs/2011.08042, 2020. 1
- [15] Ang Li, Shijie Sun, Zhaoyang Zhang, Mingtao Feng, Chengzhong Wu, and Wang Li. A multi-scale traffic object detection algorithm for road scenes based on improved yolov5. *Electronics*, 12(4):878, 2023. 6, 7
- [16] Yuhang Li, Yufei Guo, Shanghang Zhang, Shikuan Deng, Yongqing Hai, and Shi Gu. Differentiable spike: Rethinking gradient-descent for training spiking neural networks. In *Advances in Neural Information Processing Systems*, pages 23426–23439. Curran Associates, Inc., 2021. 6
- [17] T-Y. Lin, M. Maire, S. Belongie, J. Hays, P. Perona, D. Ramanan, P. Dollár, and C. L. Zitnick. Microsoft coco: Common objects in context. In *European conference on computer vision*, pages 740–755. Springer, 2014. 4
- [18] Yahui Liu, Enver Sangineto, Wei Bi, Nicu Sebe, Bruno Lepri, and Marco Nadai. Efficient training of visual transformers with small datasets. *Advances in Neural Information Processing Systems*, 34:23818–23830, 2021. 6
- [19] Ze Liu, Yutong Lin, Yue Cao, Han Hu, Yixuan Wei, Zheng Zhang, Stephen Lin, and Baining Guo. Swin transformer: Hierarchical vision transformer using shifted windows, 2021. 6
- [20] I. Loshchilov and F. Hutter. Fixing weight decay regularization in adam, 2018. 1
- [21] L. Luo, Y. Xiong, Y. Liu, and X. Sun. Adaptive gradient methods with dynamic bound of learning rate. *CoRR*, abs/1902.09843, 2019. 1
- [22] P. G. Mulloy. Smoothing data with faster moving averages. *Technical Analysis of Stocks & Commodities*, 1994. 1
- [23] B. T. Polyak. Some methods of speeding up the convergence of iteration methods. *USSR computational Mathematics and Mathematical Physics*, 1964. 8
- [24] N. Qian. On the momentum term in gradient descent learning algorithms. *Neural networks : the official journal of the International Neural Network Society*, 12 1:145–151, 1999. 1
- [25] S. J. Reddi, S. Kale, and S. Kumar. On the convergence of adam and beyond, 2019. 1
- [26] Tal Ridnik, Emanuel Ben-Baruch, Asaf Noy, and Lihi Zelnik-Manor. Imagenet-21k pretraining for the masses, 2021. 6
- [27] H. Robbins and S. Monro. A stochastic approximation method. *The annals of mathematical statistics*, pages 400–407, 1951. 1
- [28] O. Russakovsky, J. Deng, H. Su, J. Krause, S. Satheesh, S. Ma, Z. Huang, A. Karpathy, A. Khosla, M. Bernstein, A. C. Berg, and L. Fei-Fei. ImageNet Large Scale Visual Recognition Challenge. *International Journal of Computer Vision (IJCV)*, 115(3):211–252, 2015. 4
- [29] Mohd Sadiq, Sarfaraz Masood, and Om Pal. Fd-yolov5: A fuzzy image enhancement based robust object detection model for safety helmet detection. *International Journal of Fuzzy Systems*, 24, 2022. 6, 7
- [30] Christian Szegedy, Vincent Vanhoucke, Sergey Ioffe, Jonathon Shlens, and Zbigniew Wojna. Rethinking the inception architecture for computer vision, 2015. 6
- [31] Mingxing Tan and Quoc V. Le. Efficientnet: Rethinking model scaling for convolutional neural networks. *CoRR*, abs/1905.11946, 2019. 6
- [32] T. Tieleman and G. Hinton. Lecture 6.5—RmsProp: Divide the gradient by a running average of its recent magnitude. COURSERA: Neural Networks for Machine Learning, 2012. 1
- [33] Haiping Wu, Bin Xiao, Noel Codella, Mengchen Liu, Xiyang Dai, Lu Yuan, and Lei Zhang. Cvt: Introducing convolutions to vision transformers, 2021. 6
- [34] Z. Yao, A. Gholami, S. Shen, M. Mustafa, K. Keutzer, and M. Mahoney. Adahessian: An adaptive second order optimizer for machine learning. In *proceedings of the AAAI conference on artificial intelligence*, pages 10665–10673, 2021. 1
- [35] Weihao Yu, Chenyang Si, Pan Zhou, Mi Luo, Yichen Zhou, Jiashi Feng, Shuicheng Yan, and Xinchao Wang. Metaformer baselines for vision. *IEEE Transactions on Pattern Analysis and Machine Intelligence*, 46(2):896–912, 2024. 6
- [36] Li Yuan, Yunpeng Chen, Tao Wang, Weihao Yu, Yujun Shi, Zihang Jiang, Francis EH Tay, Jiashi Feng, and Shuicheng Yan. Tokens-to-token vit: Training vision transformers from scratch on imagenet, 2021. 6
- [37] Sergey Zagoruyko and Nikos Komodakis. Wide residual networks, 2017. 6
- [38] M. D. Zeiler. Adadelta: An adaptive learning rate method, 2012. 1